npg

# Phospholipase D-mediated autophagic regulation is a potential target for cancer therapy

YH Jang[1,3], KY Choi[2] and DS Min*[1,2]

Autophagy is a catabolic process in which cell components are degraded to maintain cellular homeostasis by nutrient limitations. Defects of autophagy are involved in numerous diseases, including cancer. Here, we demonstrate a new role of phospholipase D (PLD) as a regulator of autophagy. PLD inhibition enhances autophagic flux via ATG1 (ULK1), ATG5 and ATG7, which are essential autophagy gene products critical for autophagosome formation. Moreover, PLD suppresses autophagy by differentially modulating phosphorylation of ULK1 mediated by mTOR and adenosine monophosphate-activated protein kinase (AMPK), and by suppressing the interaction of Beclin 1 with vacuolar-sorting protein 34 (Vps34), indicating that PLD coordinates major players of the autophagic pathway, AMPK-mTOR-ULK1 and Vps34/Beclin 1. Ultimately, PLD inhibition significantly sensitized in vitro and in vivo cancer regression via genetic and pharmacological inhibition of autophagy, providing rationale for a new therapeutic approach to enhancing the anticancer efficacy of PLD inhibition. Collectively, we show a novel role for PLD in the molecular machinery regulating autophagy.

Autophagy is a tightly regulated process through which organelles and proteins are sequestered into autophagic vesicles (autophagosome) within cytosol.[1] These vesicles then fuse with the lysosome, forming autophagolysosomes, which promote the degradation of intracellular contents. Expansion of autophagosomes involves the recruitment of microtubule-associated protein light chain 3 (LC3-I), which is cleaved and lipidated during the initiation of autophagy. This lipidated LC3-II translocates to and associates with the autophagosome in a punctate pattern,[2] and remains on mature autophagosomes until after fusion with lysosomes; accordingly, it is commonly used to monitor autophagy.[3]

Autophagy is crucial to maintenance of cellular nutrient and energy homeostasis and essential to normal development.[4] Defects in autophagy are closely associated with numerous human diseases, including cancer.[5,6] In a tumor microenvironment, autophagy can promote cancer cell survival in response to metabolic stress.[7] However, progressive autophagy can also induce cell death, and human cancers often display inactivating mutations in autophagy-promoting genes.[8] Thus, autophagy is a double-edged sword in tumorigenesis, acting both as a tumor suppressor and a protector of cancer cell survival; accordingly, elucidation of its exact role at different stages of cancer progression and in treatment responsiveness is a complex and challenging task.

A series of protein complexes composed of autophagy-related gene (Atg gene) products coordinates the formation of autophagosomes. The ATG1/ULK1 complex (Atg1 in yeast and ULK1 in mammals) is an essential positive regulator of autophagosome formation.[9] mTOR serves as a major intracellular hub for integration of autophagy-related signals.[10] mTOR inhibits autophagy initiation by phosphorylating ULK1Ser 757.[11] Upstream of mTOR is the cellular energy-sensing pathway controlled by adenosine monophosphate-activated protein kinase (AMPK).[10] Under glucose starvation, activated AMPK inhibits mTOR to relieve the phosphorylation of ULK1 Ser757, leading to ULK1-AMPK interaction.[11] AMPK then phosphorylates ULK1 on Ser555, Ser 317 and Ser777, activates ULK1 kinase, and eventually leads to the induction of autophagy.[11,12] Autophagy is also regulated by Beclin 1 (Atg6), which forms a complex with vacuolar-sorting protein 34 (Vps34), a class III phosphatidylinositol 3-kinase, and serves as a platform for recruitment of other autophagy-related proteins that are critical to autophagosome formation.[13] Bcl-2 possesses anti-autophagy function in addition to apoptosis inhibition via physical interaction with Beclin 1.[14] During nutrient starvation, JNK1-mediated Bcl-2 phosphorylation dissociates Beclin1/Bcl-2 complex and induces autophagy.[15]

Mitogenic activation of mTOR requires the lipid second messenger phosphatidic acid (PA), which binds to mTOR.[16,17] Phospholipase D (PLD), which catalyzes the hydrolysis of phosphatidylcholine to PA, has been established as a key upstream component in the mitogenic mTOR pathway.[18,19] Given the central role for PLD in cell survival,

it is not surprising that PLD dysregulation has been implicated in various cancers.[18,19] Despite the implications of PLD and autophagy in cancer-related processes, current evidence linking these two fields of research is severely limited.

In the present study, we show that PLD1 as a new regulator of autophagy, coordinates major players of the autophagic pathway, AMPK-mTOR-ULK1 and the Vps34/Beclin 1 signaling pathway. PLD inhibition promotes autophagic flux. Moreover, PLD1 inhibitor sensitized *in vitro* and *in vivo* cancer regression induced by genetic and pharmacological inhibition of autophagy. Our findings suggest that regulation of autophagy signaling networks via PLD1 inhibition provide rationale for a new therapeutic approach to augment the efficacy of anticancer regimens.

## Results

**PLD1 suppresses autophagy.** To examine the involvement of PLD1 in autophagy, we used RNA interference against PLD1. Depletion of PLD1 significantly induced autophagy in HEK293 and HeLa cells, as indicated by punctate dots of endogenous LC3 (Figure 1a). p62 is a protein sequestered in autophagosomes that is lost when autophagosomes fuse with lysosomes. Thus, an increase of
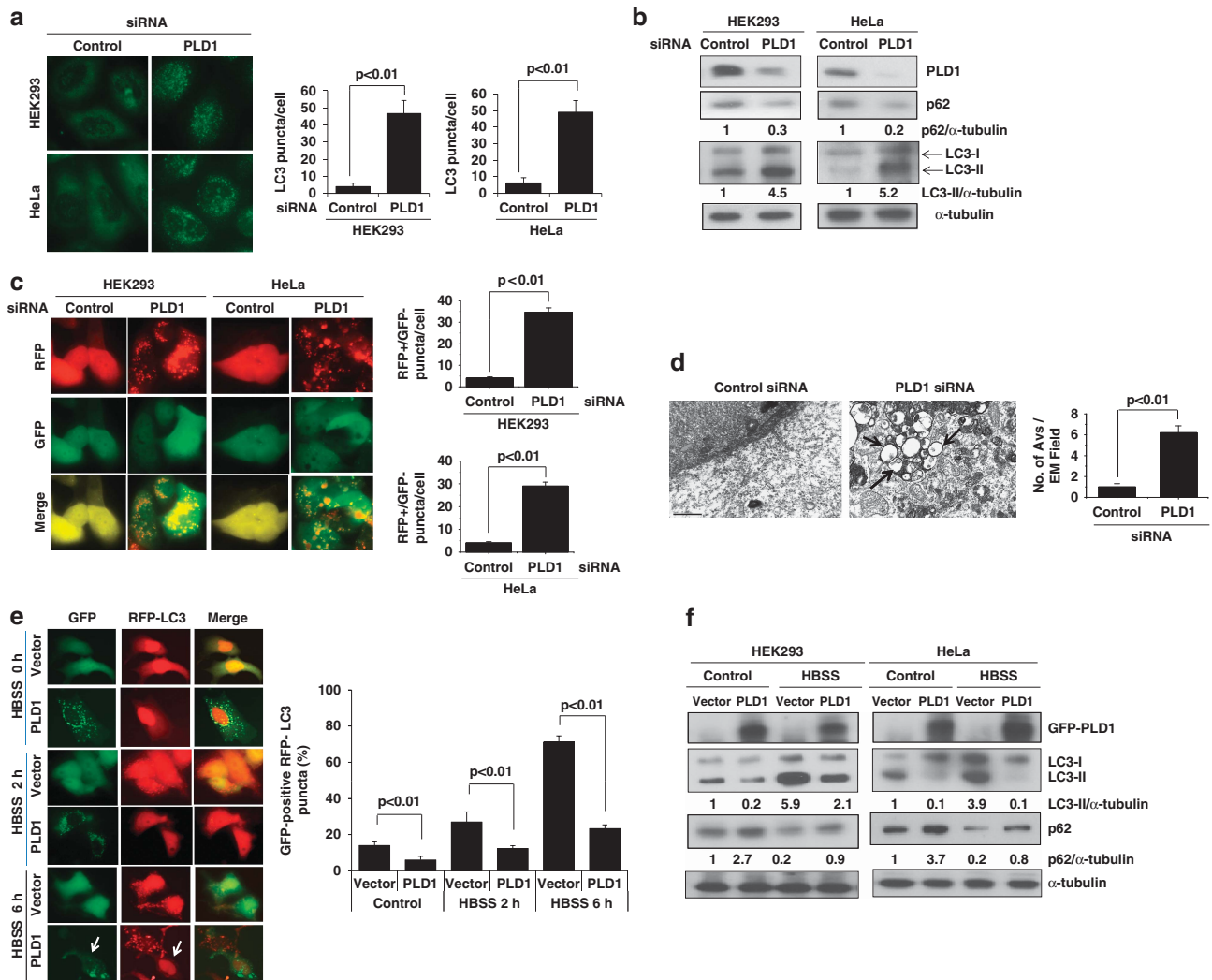


**Figure 1** PLD1 suppresses both basal and starvation-induced autophagy. (**a**) HEK293 and HeLa cells were transfected with siRNAs for a control or PLD1, then immunostained with antibody to LC3. Endogenous LC3 punctate dots were observed by fluorescence microscopy and quantification of the number of LC3 puncta per cell (three to five cells were counted). Data are representative of three independent experiments. (**b**) The cells were transfected with siRNA for PLD1. The lysates were then immunoblotted with the indicated antibodies. The levels of p62 or LC3-II to α-tubulin were quantified by densitometer analysis. (**c**) Cells were transfected with mRFP-GFP-LC3 and the indicated siRNA for 24 h. The total numbers of RFP-positive/GFP-negative puncta per cell were counted. (**d**) HeLa cells were transfected with the indicated siRNA and then fixed and examined by transmission electron microscopy for autophagicvacuoles (AVs). Quantifications based on counting autophagic vacuoles in the field of view. The values are the mean ± S.D. of three independent experiments. (**e**) HeLa cells were co-transfected with GFP or GFP-PLD1 and RFP-LC3 and then cultured under amino acid and serum starvation conditions (HBSS media) for 2 or 6 h, after which the percentage of RFP punctate cells relative to the percentage of GFP-expressing cells was determined. White arrows indicate GFP-PLD1 expressing non-punctate cells. The values are the mean ± S.D. of three independent experiments. (**f**) HeLa cells were transfected with GFP-PLD1 or GFP vector and then cultured with or without HBSS medium for 6 h. The lysates were immunoblotted with the indicated antibody and the levels of p62 or LC3-II relative to α-tubulin were quantified by densitometer analysis. Data are representative of three independent experiments

p62 indicates inhibition of autophagy.[20] PLD1 depletion increased the level of LC3-II and reduced the level of p62 protein (Figure 1b). Moreover, the maturation process through which autophagosomes are converted into autolysosomes can be monitored by the monomeric red fluorescent protein (mRFP)-GFP tandem fluorescent-tagged LC3 (tfLC3) method.[21] The GFP-LC3 punctate feature of mRFP-GFP tandem autophagy flux reporter is not detectable in the acidic pH lysosomal environment by lysosomal hydrolysis, whereas the mRFP-LC3 punctate feature is still detectable. Our data showed that knockdown of PLD1 significantly increased the transition of RFP-GFP/LC3-positive autophagosomes to RFP-positive, GFP-negative autolysosomes in RFP-GFP/LC3-transfected cells (Figure 1c), suggesting that depletion of PLD1 promotes autophagic flux. We further examined the effect of PLD1 on autophagic flux, based on the ratio of wild type and autophagy-deficient mutant of renilla luciferase RLuc-LC3 (LC3$^{WT}$/LC3$^{G120A}$).[22,23] Both knockdown and inhibition of PLD1 effectively induced autophagy as evident from the ratio of luciferase activity of the two RLuc-LC3s (Supplementary Figures 1a and b). In addition, overexpression of PLD1 significantly suppressed autophagic flux during 2 or 6 h of starvation (Supplementary Figure 1c). These data strengthen that PLD1 inhibition promotes autophagy flux. Furthermore, PLD1 depletion revealed a significant increase in the number of autophagic vacuoles as analyzed by transmission electron microscopy (TEM; Figure 1d). We also observed autophagy proceeding in PLD1 knockout mouse embryonic fibroblasts (MEFs; Supplementary Figures 2a and b). Ectopic expression of GFP-PLD1 decreased autophagy induced by 2 or 6 h of starvation, as measured by the accumulation of GFP-positive RFP-LC3 puncta (Figure 1f). In addition, overexpression of PLD1 reduced the level of LC3-II and increased the level of p62 (Figure 1g). Moreover, LC3-II induced by silencing of PLD1 was suppressed by overexpression of PLD1 (Supplementary Figure 3). We measured the degradation of long-lived proteins in PLD1-depleted cells. This assay provides a functional readout as autophagy is the major pathway through which many of these proteins are degraded. Significant increase in the degradation of long-lived proteins was detected by PLD1-depleted cells, compared with that of control siRNA cells (Supplementary Figure 4), demonstrating that knock-down of PLD1 stimulates the autophagic pathway with increased protein turnover. Endogenous and exogenous PLD1 activity were increased for 2 h of starvation and thereafter (6 h, 12 h) decreased (Supplementary Figure 5). Thus, it seems that decreased activity of PLD1 for prolonged starvation promotes autophagy. In addition, ectopic expression of PLD2 suppressed autophagy as measured by the accumulation of GFP-positive RFP-LC3 puncta (Supplementary Figure 6). Taken together, these results suggest that PLD1 negatively regulates autophagy.

**Enzymatic activity of PLD is involved in the regulation of autophagy.** To examine whether PLD activity is involved in autophagy, we co-transfected RFP-LC3 with wild-type GFP-PLD1 or a catalytically inactive mutant form of PLD1, GFP-PLD1$^{K898R}$(KRM-PLD1). Expression of PLD1$^{wt}$, but not PLD1$^{K898R}$, significantly inhibited GFP-positive RFP-LC3

puncta formation (Figure 2a), suggesting the involvement of PLD activity in the regulation of autophagy. Moreover, PA significantly suppressed starvation-induced autophagy as analyzed by mRFP-GFP tandem LC3 punctate (RFP-positive, GFP-negative puncta) formation (Figure 2b) and LC3-II level in HeLa cells (Figure 2c). Furthermore, PLD1 inhibition significantly increased autophagy under both basal conditions and starvation (Figure 2d). PA suppressed PLD1 inhibitor-induced autophagy (Supplementary Figure 7). Under basal conditions, PLD1 inhibition enhanced the level of LC3-II protein in a variety of cells (Figure 2e), suggesting that PLD1 inhibitor-induced autophagy is a general phenomenon. In addition, PLD inhibition increased the level of LC3-II protein in a dose- or time-dependent manner (Supplementary Figure 8), and increased the formation of autophagic vacuoles as analyzed by TEM (Figure 2f). The accumulation of LC3-II is not only a consequence of the LC3-I to LC3-II conversion, but also of an increase in LC3 synthesis. Thus, we examined whether PLD1 affects expression level of LC3 during starvation. Although starvation of 2 and 6 h induced mRNA level of LC3, ectopic expression of PLD1 and PLD1 inhibition did not affect expression of LC3 (Supplementary Figure 9). Taken together, these data indicate that the enzymatic activity of PLD1 is involved in the inhibition of autophagy.

**Mechanisms of enhanced autophagic vacuolization by PLD1 inhibition.** To understand the regulation of the autophagic pathway by PLD1, we examined whether PLD1 inhibition is dependent on *Atg* genes. To accomplish this, we used isogenic MEF deficient for the essential autophagy genes, *Atg5* or *Atg7,* which were completely defective for autophagy.[24,25] RFP-LC3 puncta and LC3-II level induced by knockdown of PLD1 or PLD1 inhibition were dramatically suppressed in *Atg5* and *Atg7* null MEF (Figures 3a–d). The accumulation of autophagosomes and autolysosomesin response to inhibition or depletion of PLD1 could involve enhanced autophagic sequestration (on-rate) or reduced degradation of autophagic material by fusion with lysosomes (off-rate). To distinguish between these possibilities, we assessed PLD1 inhibitor-induced autophagic vacuolization by monitoring colocalization of the autophagic marker, GFP-LC3, with the lysosomal marker, Lamp-1, in the presence or absence of bafilomycin A1 (Baf A1), which is known to inhibit fusion between autophagosomes and lysosomes.[3] PLD1 inhibitor, but not Baf A1, induced colocalization between Lamp-1 and LC3, suggesting that autophagosomes encounter lysosomes in PLD1 inhibitor-treated cells (Figure 3e). In addition, PLD1 inhibitor but not Baf A1 increased autophagic flux as measured by the formation of RFP-positive, GFP-negative puncta (Supplementary Figure 10a). However, exogenous PLD1 significantly suppressed the colocalization between Lamp-1 and LC3 under both 2 and 6 h of starvation conditions (Supplementary Figure 10b). To obtain a better determination of the inhibitory effect of PLD1 on the formation of autophagosomes, we analyzed the kinetics of LC3-II synthesis. Overexpression of PLD1 greatly reduced LC3-II biosynthesis by Baf A1 treatment at two time points, compared with that of control cells, indicating that fewer autophagsomes are formed in cells overexpressing PLD1,
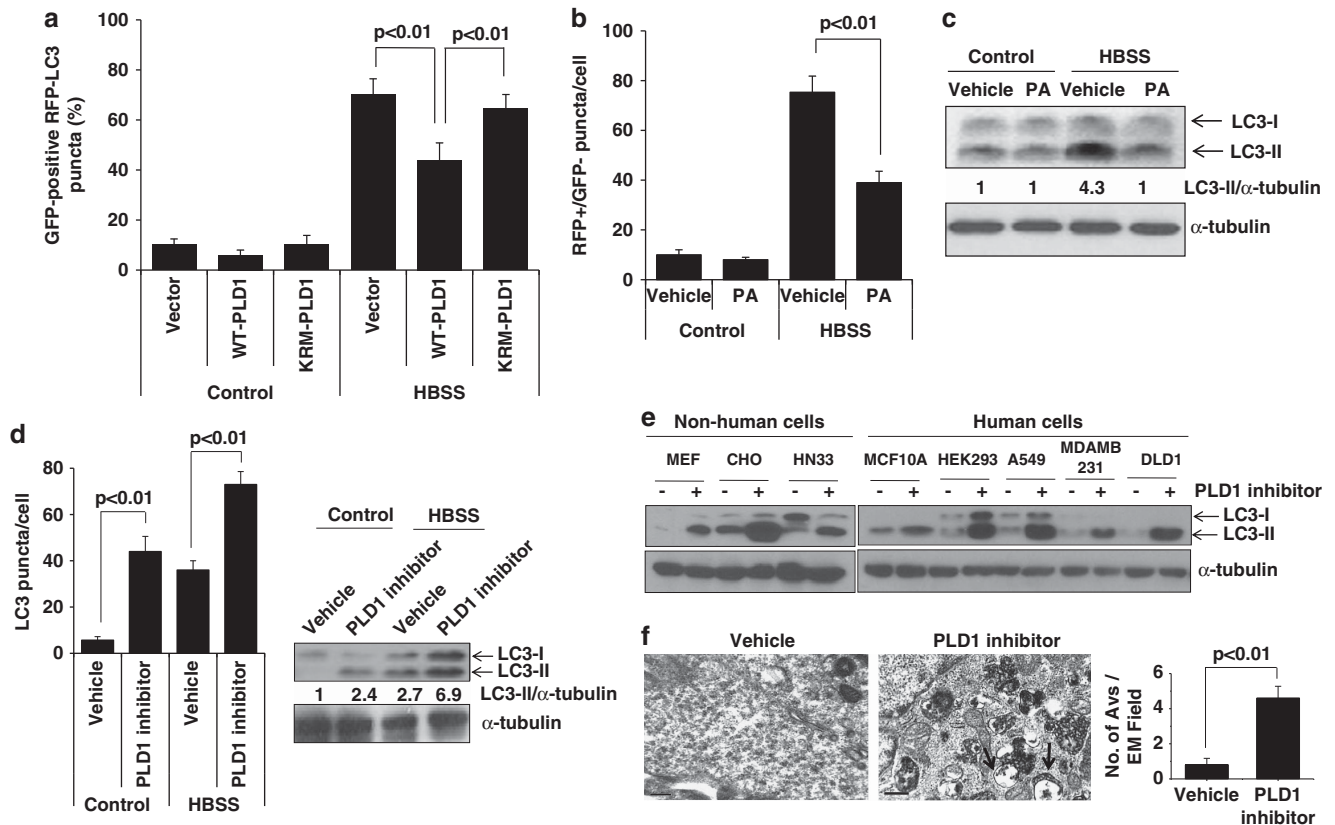
**Figure 2** Enzymatic activity of PLD is involved in the regulation of autophagy. (**a**) HeLa cells were co-transfected with GFP vector, GFP-WT-PLD1 or GFP-KRM-PLD1 and RFP-LC3 and then cultured in HBSS or normal medium for 6 h, after which the percentage of RFP punctate cells relative to the percentage of GFP-expressing cells was determined. Data are representative of three independent experiments. (**b**) HeLa cells were transfected with mRFP-GFP-LC3 and then pretreated with or without PA (50 $\mu$M) for 1 h, after which the cells were cultured in normal or HBSS medium for 12 h. Autolysosomes were quantified by counting RFP-positive/GFP-negative puncta per cell (three to five cells were counted). (**c**) HeLa cells were treated with or without PA (50 $\mu$M) for 1 h, then starved by culture in HBSS medium for 6 h, after which the lysates were analyzed by immunoblot using the indicated antibodies. The level of LC3-II to $\alpha$-tubulin was quantified by densitometer analysis. (**d**) HeLa cells were pre-treated with or without PLD1 inhibitor (10 $\mu$M) and then cultured in normal or HBSS medium for 6 h. The cells were then fixed, permeabilized and stained with a Texas Red-conjugated antibody specific for endogenous LC3, and the number of LC3 puncta per cell was counted (three to five cells were counted). The lysates were immunoblotted with the indicated antibody. The levels of LC3-II to $\alpha$-tubulin were quantified by densitometer analysis. (**e**) Various cells were pre-treated with or without PLD1 inhibitor (10 $\mu$M) for 12 h, after which the lysates were analyzed by immunoblot using the indicated antibodies. (**f**) HeLa cells were treated with or without PLD1 inhibitor and then fixed and examined by transmission electron microscopy for autophagic vacuoles. Quantification is based on counting of autophagic vacuoles in the field of view. The values are the mean ± S.D. of three independent experiments. Arrows indicate autophagic vacuoles

and thus PLD1 has an inhibitory effect on autophagosome formation (Supplementary Figure 10c). Furthermore, Baf A1 increased the PLD1 inhibitor-triggered induction of LC3-II (Figure 3f). These data suggest that PLD1 inhibition increases the on-rate of autophagy, at least *in vitro*.

**PLD1 regulates autophagy through mTOR/AMPK/ULK1-mediated pathways and modulation of interaction of Vps34 with Beclin-1.** Autophagy is controlled by several kinases including mTOR, a negative regulator of autophagy,[26] and AMPK, a positive regulator of autophagy.[27] PLD1 depletion suppressed the phosphorylation of mTOR and S6K, a downstream target of mTOR (Figure 4a, left panel). Moreover, PLD1 inhibitor suppressed activation of mTOR and S6K (Figure 4a, right panel). Overexpression of PLD1 recovered the phosphorylation of mTOR and S6K reduced by nutrient starvation (Figure 4b). Inhibition of mTOR kinase by rapamycin and PLD1 inhibitor induced autophagy as indicated

by mRFP-GFP tandem LC3 punctate formation (Figure 4c). Cotreatment did not further increase autophagy, compared with that of each treatment, suggesting that PLD1 inhibition induces autophagy through the mTOR-mediated pathway. Interestingly, PLD1 inhibition increased both phosphorylation of AMPK (Thr172) and phosphorylation of ULK1 Ser555, which is mediated by AMPK, in a time-dependent manner, whereas PLD1 inhibition suppressed phosphorylation of ULK1 Ser757 mediated by mTOR (Figure 4d). We further used siRNA approach to exclude an off-target effect of the inhibitor. The effect of PLD1 siRNA on the phosphorylation of AMPK and ULK1 was comparable with that of PLD1 inhibition (Figure 4e). Moreover, PLD1 inhibition dramatically suppressed the level of LC3-II (Figure 4f) and RFP-LC3 puncta in Ulk1$^{-/-}$ MEF (Figure 4g). These data suggest that PLD1 inhibition induces autophagy through activation of AMPK-ULK1 (Ser555 phosphorylation) and suppression of mTOR-ULK1 (Ser757 phosphorylation).
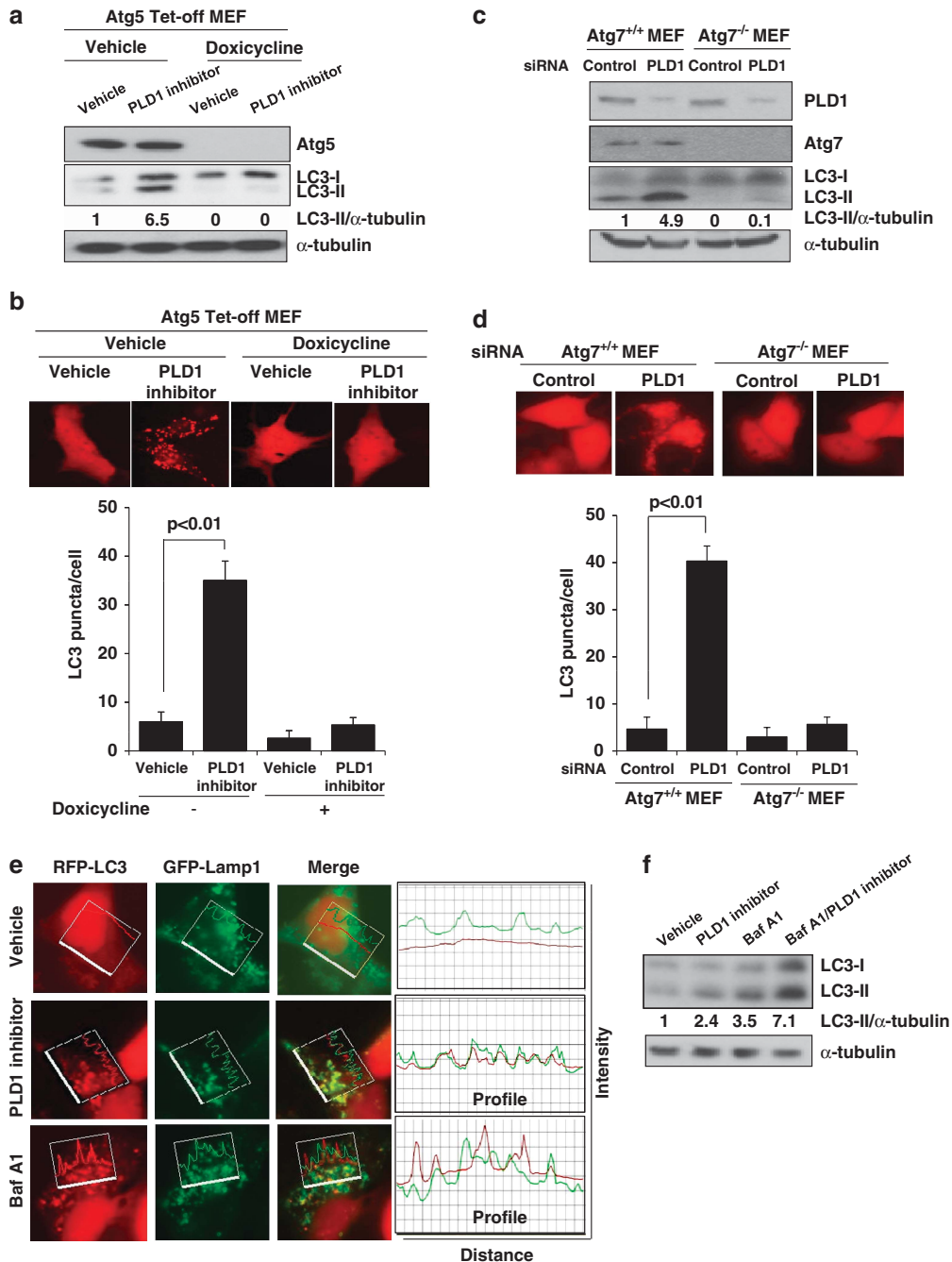
**Figure 3** Mechanisms of enhanced autophagic vacuolization by PLD1 inhibition. (**a**) Atg5 Tet-off MEFs were treated with or without 10 ng/ml of doxycycline for 24 h and with or without PLD1 inhibitor (10 $\mu$M) for 4 h, after which the lysates were immunoblotted with the indicated antibodies. (**b**) Atg5 Tet-off MEF were treated with or without 10 ng/ml of doxycycline for 24 h, then transfected with RFP-LC3, followed by treatment with PLD1 inhibitor. RFP-LC3 punctate dot cells were observed by fluorescence microscopy and the number of RFP punctate cells was quantified using the methods shown in the legend of Figure 2. The values are the mean ± S.D. of three independent experiments. (**c**) Two isogenic MEF cell lines (Atg7$^{+/+}$ and Atg7$^{-/-}$) were transfected with the indicated siRNA and the lysates were then immunoblotted with the indicated antibodies. (**d**) The cells were transfected with RFP-LC3 for 24 h and then transfected with siRNA for PLD1 for 24 h. RFP-LC3 punctate dot cells were observed by fluorescence microscopy and the number of RFP punctate cells was quantified. (**e**) HeLa cells were co-transfected with RFP-LC3 and GFP-Lamp1, then pretreated with Baf A1 (100 nM) or PLD1 inhibitor (10 $\mu$M) for 8 h. The colocalization between GFP-LC3 and Lamp-1 was analyzed. Representative fluorescence microphotographs are shown together with the profiles of colocalization. (**f**) HeLa cells were treated with PLD1 inhibitor and/or Baf A1 for 8 h, after which the lysates were immunoblotted with the indicated antibody. Data are representative of three independent experiments

Beclin 1 has a critical role in the initiation of autophagy and its complex interactome has a major effect on the positive and negative regulation of autophagy.[28] Bcl-2 interacts with

Beclin 1 and suppresses autophagy.[14] Importantly, the phosphorylation status of Bcl-2 can interfere with this autophagy-regulating interaction. JNK1-mediated Bcl-2
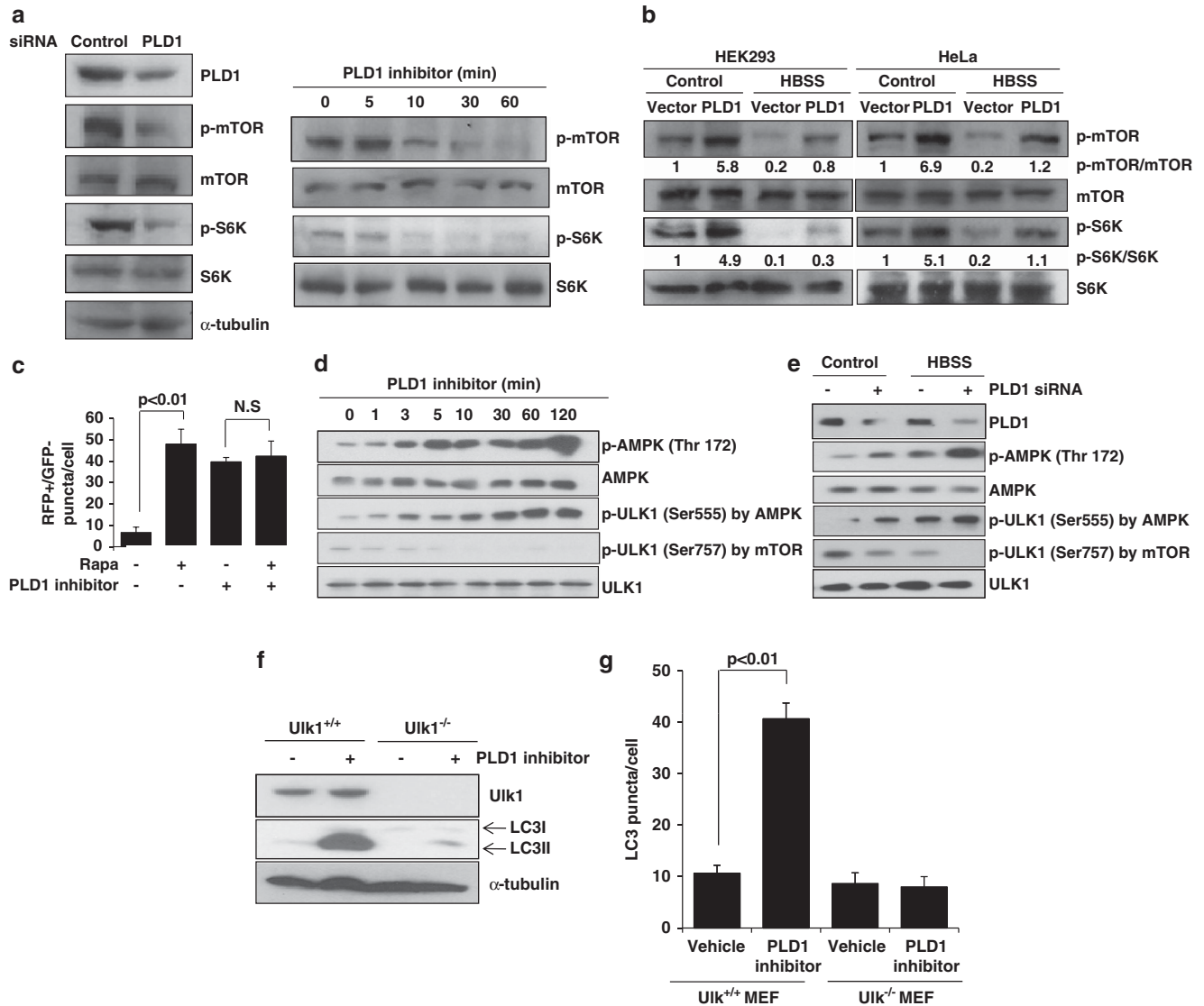
**Figure 4** PLD1 activity is involved in the regulation of autophagy through mTOR/AMPK/ULK1-mediated pathways.(**a**) HeLa cells were transfected with siRNAs for control or PLD1 and the lysates were immunoblotted with the indicated antibodies (left panel). The cells were treated with PLD1 inhibitor (10 $\mu$M) for the indicated time and the lysates were immunoblotted with the indicated antibodies.(**b**) The cells were transfected with empty vectors or PLD1 and then cultured in normal or HBSS medium for 6 h, after which the lysates were immunoblotted with the indicated antibodies. The ratios of the phosphorylated form to the total form were quantified by densitometer analysis. Data are representative of three independent experiments. (**c**) HeLa cells were transfected with mRFP-GFP-LC3 and treated with or without PLD1 inhibitor (10 $\mu$M) or rapamycine (1 $\mu$M) for 8 h. Autolysosomes were quantified by counting RFP-positive/GFP-negative puncta per cell (three to five cells were counted).The values are the mean $\pm$ S.D. of three independent experiments. (**d** and **e**) HeLa cells were treated with PLD1 inhibitor (10 $\mu$M) or PLD1 siRNA for the indicated time or starvation (6 h) and complete media and the lysates were immunoblotted with the indicated antibodies. (**f**) Two isogenic MEF cells (Ulk1 $^{+/+}$ and Ulk1-null) were treated with PLD1 inhibitor and the lysates were immunoblotted by the indicated antibodies. (**g**) The cells were transfected with RFP-LC3, followed by treatment with PLD1 inhibitor. RFP-LC3 punctate dot cells were observed with fluorescence microscopy and the number of RFP punctate cells was quantified. The values are the mean $\pm$ S.D. of three independent experiments

phosphorylation dissociates Beclin 1/Bcl-2 complex and induces autophagy.[13]

PLD1 inhibition greatly increased phosphorylation of JNK and disrupted the interaction between exogenous and endogenous Beclin 1 and Bcl2 in complete media (Figures 5a and b). PA decreased phosphorylation of JNK and increased endogenous association of Beclin 1 with Bcl-2 in starved cells (Figure 5c). Overexpression of PLD1 also increased interaction between these two proteins in starved

cells (Figure 5d). The interaction between Beclin 1 and Vps34 is known to induce autophagy.[29,30] PLD1 inhibition significantly increased Beclin1/Vps34 complex formation (Figure 5e), whereas expression of PLD1 greatly decreased association between Beclin 1 and Vps34 in starved cells (Figure 5f). These findings suggest that PLD1 activity is involved in regulation of the interaction of Beclin1 with Vps34 or Bcl2. Taken together, these data indicate that PLD1 suppresses autophagy through the AMPK-mTOR-ULK1-mediated
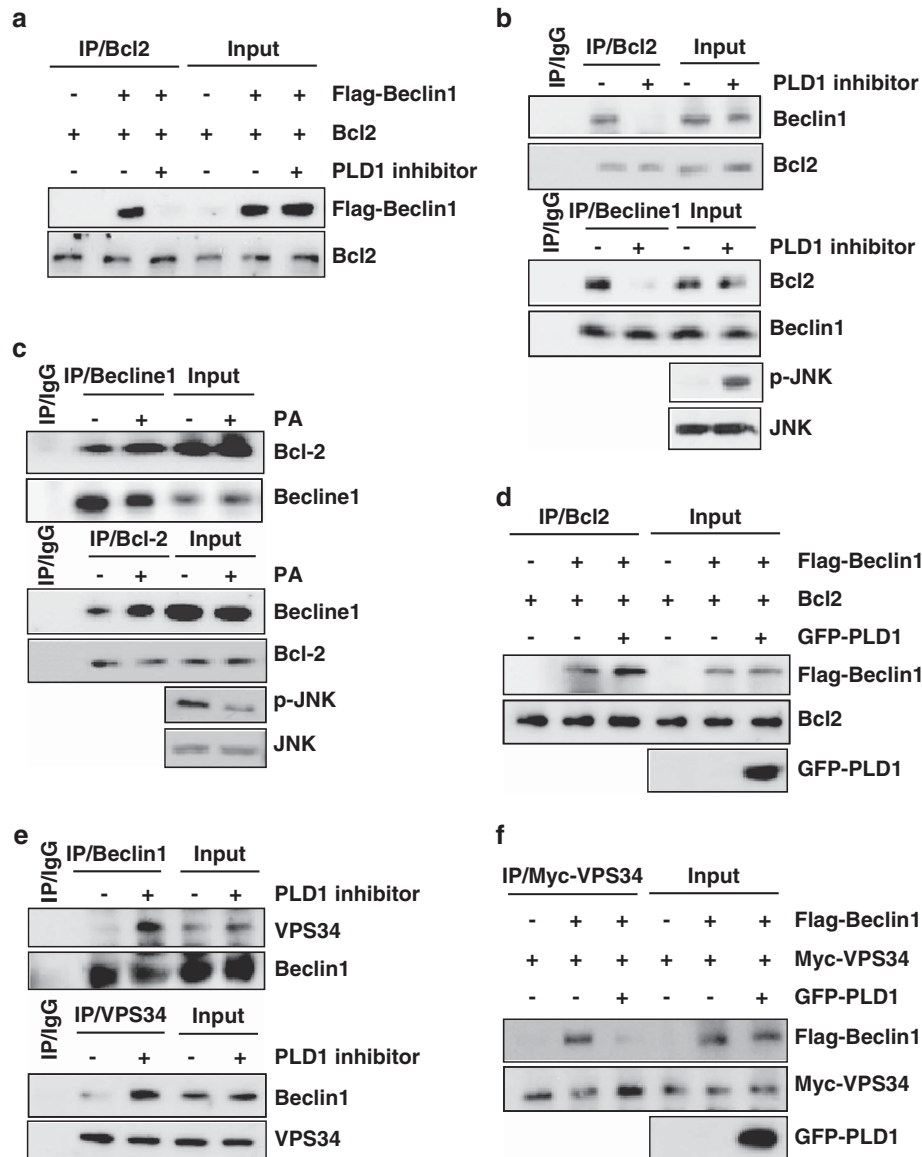
**Figure 5** PLD1 activity is required for regulation of the interaction of Beclin1 with Vps34 or Bcl2. (**a**) After cultured in complete media, HeLa cells were transfected with the indicated constructs and treated with PLD1 inhibitor (10 μM) for 1 h, after which the lysates were immunoprecipitated and/or immunoblotted using the indicated antibody. (**b**) After cultured in complete media, HeLa cells were treated with PLD1 inhibitor and co-immunoprecipitated and/or immunoblotted using the indicated antibody. (**c**) After cultured in HBSS media, HeLa cells were treated with PA (50 μM) for 1 h and co-immunoprecipitated and/or immunoblotted using the indicated antibody. (**d**) After cultured in HBSS media, HeLa cells were transfected with the indicated constructs and the lysates were immunoprecipitated and/or immunoblotted using the indicated antibody. (**e**) After cultured in complete media, HeLa cells were treated with PLD1 inhibitor and co-immunoprecipitated and/or immunoblotted using the indicated antibody. (**f**) After cultured in HBSS media, HeLa cells were transfected with the indicated constructs and the lysates were immunoprecipitated and/or immunoblotted using the indicated antibody. Data are representative of three independent experiments

pathway and modulation of the interaction of Beclin 1 with Vps34 or Bcl2.

**PLD1 inhibition sensitizes cell death via genetic and pharmacological inhibition of autophagy.** Many studies have shown that genetic knockdown of Atgs or pharmacological inhibition of autophagy can effectively enhance tumor cell death induced by diverse anticancer drugs in preclinical models.[31–33] Thus, we examined whether PLD1 inhibition induces cell death with respect to autophagy. Under starvation conditions, PLD1 inhibition significantly sensitized

cell death in Atg5$^{-/-}$ MEF (Supplementary Figure 11a). We next used Atg5$^{+/+}$ and Atg5$^{-/-}$ RasV12/T-large antigen-transformed MEF.[34] Propidium iodide (PI) staining revealed that PLD1 inhibition significantly enhanced starvation-induced cell death in Atg5$^{-/-}$RasV12/T-large antigen-transformed MEF when compared with that of Atg5$^{+/+}$ MEF (Figure 6a). PLD1 inhibition also dramatically increased caspase 3 activation in Atg5$^{-/-}$RasV12/T-large antigen-transformed MEF, but not in Atg5$^{+/+}$ MEF (Figure 6b). Moreover, PLD1 inhibition significantly increased cell death in Atg7-depleted MDA-MB231 breast cancer cells
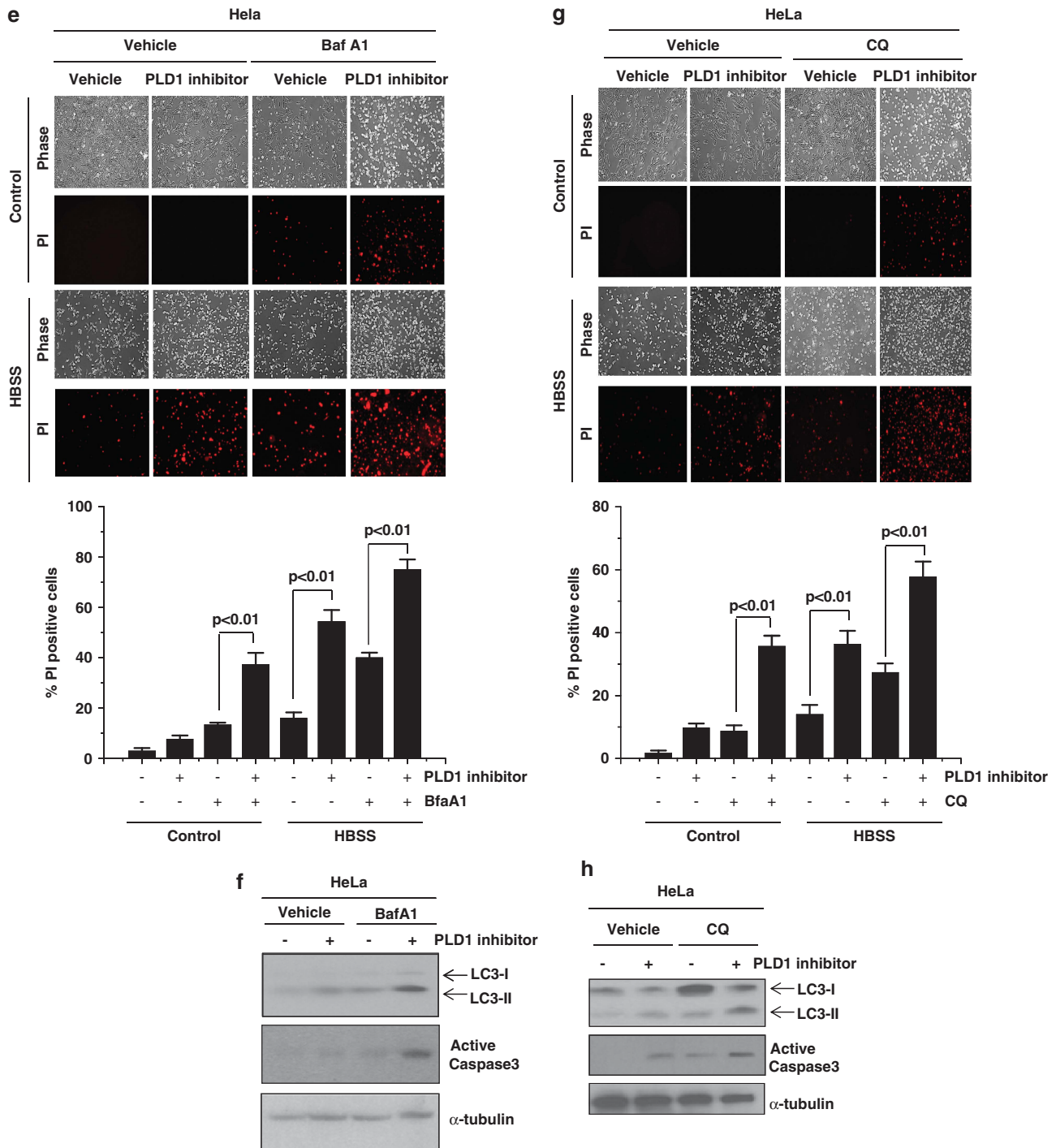
**Figure 6** (Continued)
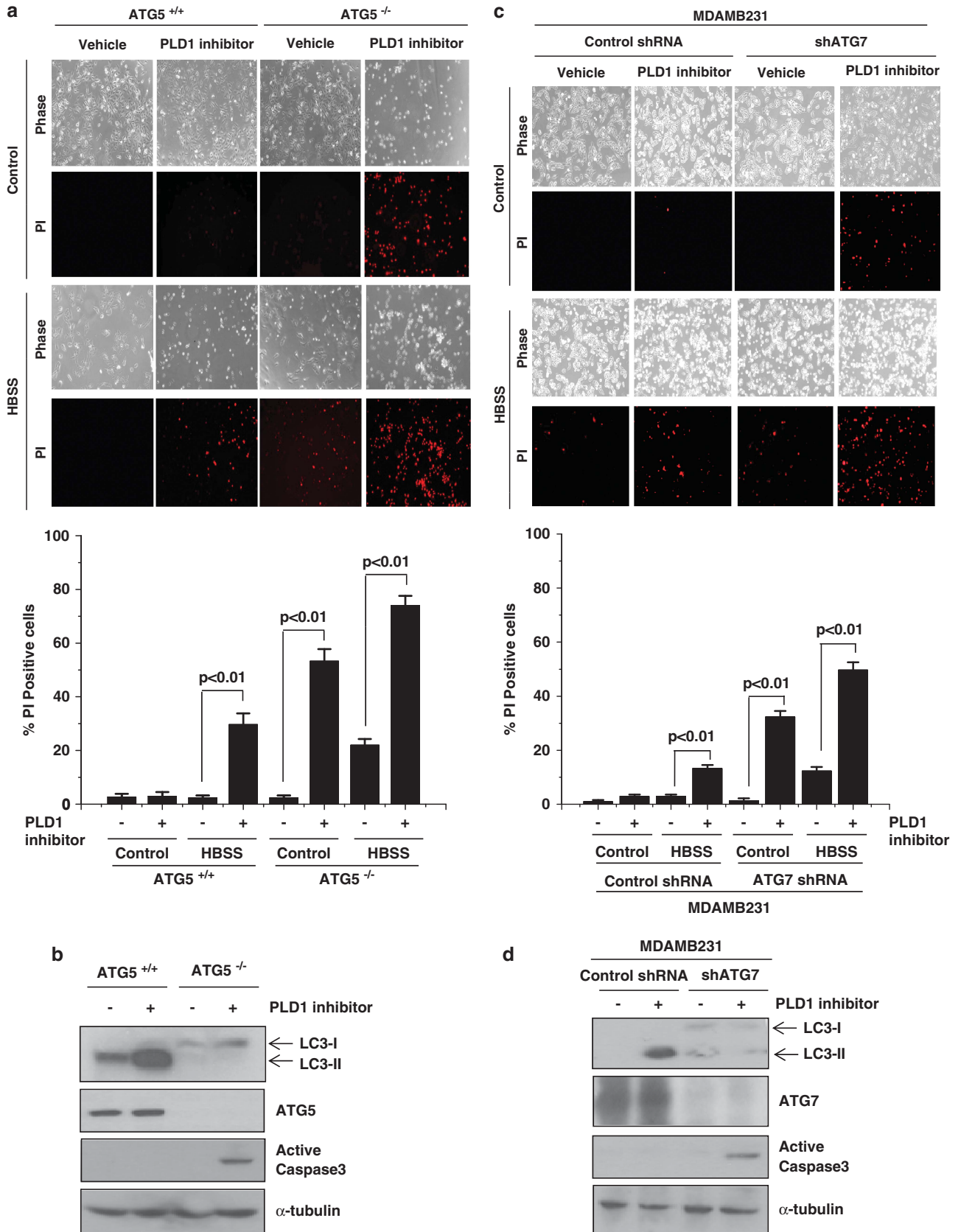
**Figure 6** PLD1 inhibition significantly sensitizes cell death by genetic and pharmacological inhibition of autophagy. (**a**) Atg5^{+/+} and Atg5^{−/−}RasV12/T-large antigen-transformed MEFs were starved with HBSS medium in the presence or absence of PLD1 inhibitor (10 $\mu$M). Cell death was determined by PI staining. The number of PI-positive cells is represented by the ratio of PI-positive cells to the overall cells (at least 100 cells were counted). The values are the mean ± S.D. of three independent experiments. (**b**) The cells were treated with PLD1 inhibitor and the lysates were immunoblotted using the indicated antibody. (**c**) The control and ATG7-depleted MDA-MB231 breast cancer cells were starved with HBSS medium in the presence or absence of PLD1 inhibitor. Cell death was determined by PI staining. The PI-positive cells were quantified as described above. The values are the mean ± S.D. of three independent experiments. (**d**) The cells were treated with PLD1 inhibitor and the lysates were immunoblotted with the indicated antibody. (**e** and **g**) HeLa cells were starved by cultivation in HBSS medium and pretreated with Baf A1 (100 nM) or CQ (50 $\mu$M) for 1 h, then treated with or without PLD1 inhibitor for 12 h. Cell death was analyzed by PI staining and quantified. The lysates from the indicated drug-treated cells were analyzed by the indicated antibody (**f** and **h**). Data are representative of three independent experiments

(Figures 6c and d). In addition, we used MEF cells lacking Atg7.[25] Comparison of the wild-type and Atg7$^{-/-}$ MEF provided a cleaner test than that using RNAi, addressing the concern for off-target effects that may plague siRNA knockdown. PLD1 inhibition significantly induced cell death in Atg7$^{-/-}$ MEF, but not Atg7$^{+/+}$ MEF (Supplementary Figure 11b). The level of LC3-II and caspase 3 activation by PLD1 inhibition in Atg7$^{-/-}$ MEF were also comparable with those of ATG7-depleted MDA-MB-231 cells (Supplementary Figure 11c). These results suggest that PLD1 inhibition increases cell death when autophagy is genetically inhibited. The inhibition of autophagy combined with chemotherapy can enhance treatment efficacy by inhibiting stress adaptation and increasing cell death. Thus, we investigated the effects of the late-stage inhibitors of autophagy, chloroquine (CQ: lysosomotropic drug that prevents acidification of the lysosomal compartment) and Baf A1. Combined treatment of HeLa cells with Baf A1 or CQ with PLD1 inhibitor significantly sensitized cell death under normal and starvation conditions (Figures 6e–h). Taken together, these data suggest that PLD1 inhibitor efficiently sensitizes cell death via genetic and pharmacological inhibition of autophagy.

**PLD1 inhibitor synergizes with genetic inhibition of autophagy and clinical inhibitor of autophagosome maturation to induce apoptosis in vivo.** To determine the in vivo relevance of PLD1 inhibitor antitumoral action with respect to autophagy, we investigated whether PLD1 inhibition promotes activation of the autophagy-mediated cell death pathway in Atg5$^{+/+}$ and Atg5$^{-/-}$RasV12/T-large antigen-transformed MEF-derived tumor xenografts. Administration of PLD1 inhibitor significantly reduced the growth and weight of tumors derived from Atg5-deficient cells when compared with that of Atg5$^{+/+}$-derived cells (Figure 7a). Furthermore, administration of PLD1 inhibitor greatly increased apoptosis in Atg5$^{-/-}$, but not in Atg5$^{+/+}$ tumors (Figures 7b–d). CQ, a drug that blocks autophagosome maturation, is a well-established clinical antimalarial agent that is also known to augment cell death and/or tumor regression.[33–35] To translate these results to an in vivo setting, we established xenografts from A549 lung cancer cells. The combination of PLD1 inhibitor and CQ led to significant tumor regression when compared with monotherapy (Figure 8a). The combination treatment induced a marked increase in apoptosis (Figures 8b and c), and reduced the expression of Ki67, a proliferation marker
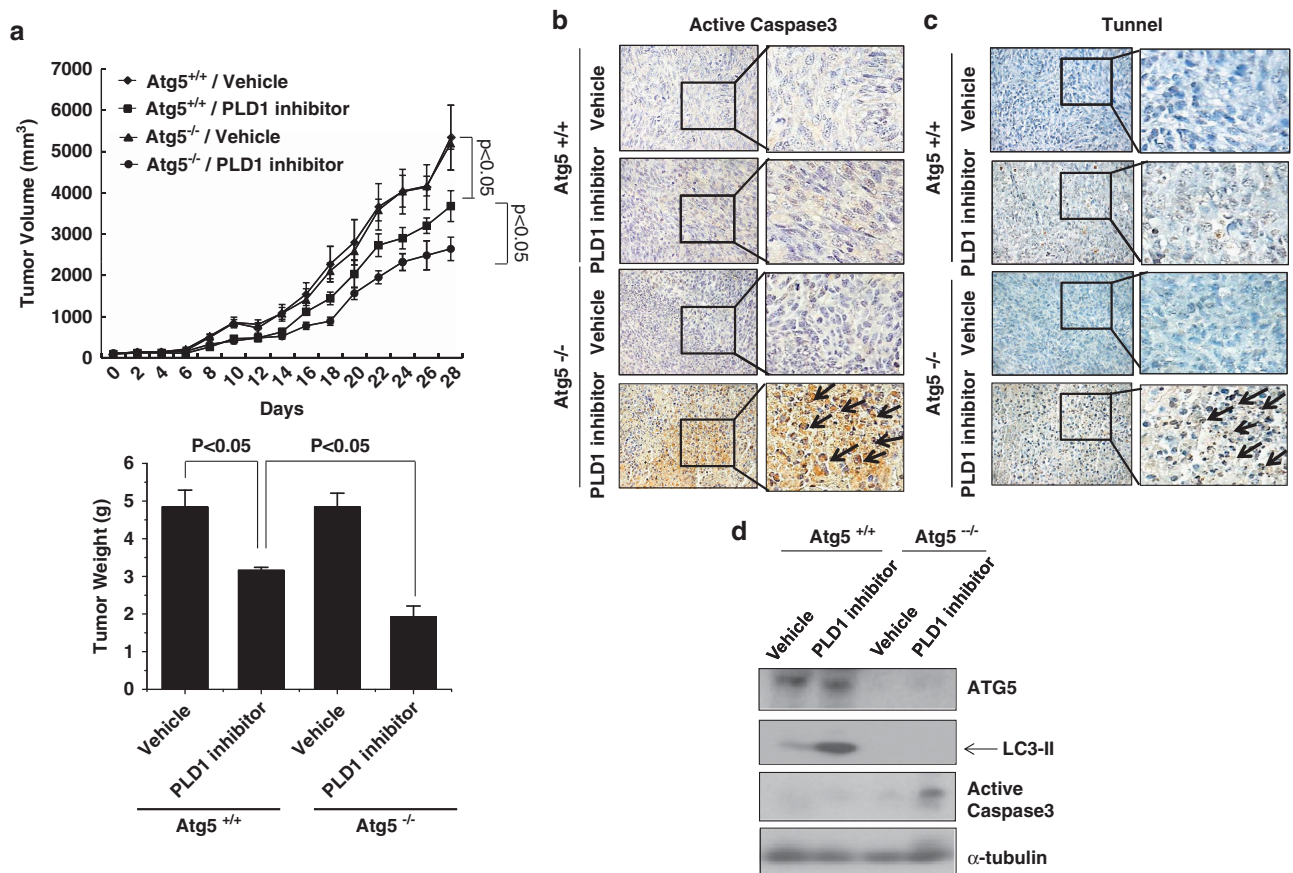


**Figure 7** PLD1 inhibitor sensitizes in vivo cancer regression via genetic inhibition of autophagy. (a) Growth inhibition of Atg5$^{+/+}$ and Atg5$^{-/-}$RasV12/T-large antigen-transformed MEF by PLD1 inhibitor (10 mg/kg, i.p., every 2 days for 4 weeks; top). The volume and weight of the tumors were measured. Data were expressed as the mean ± S.D. of seven different mice. (b and c) Immunohistochemistry of tumor tissues. Paraffin-embedded tumor sections were stained with antibody to active caspase3 and analyzed by TUNEL staining. (d) The lysates from tumor tissues were analyzed by immunoblot using the indicated antibody. Data are representative of three independent experiments. Arrows indicate active caspase or Tunnel positive cells
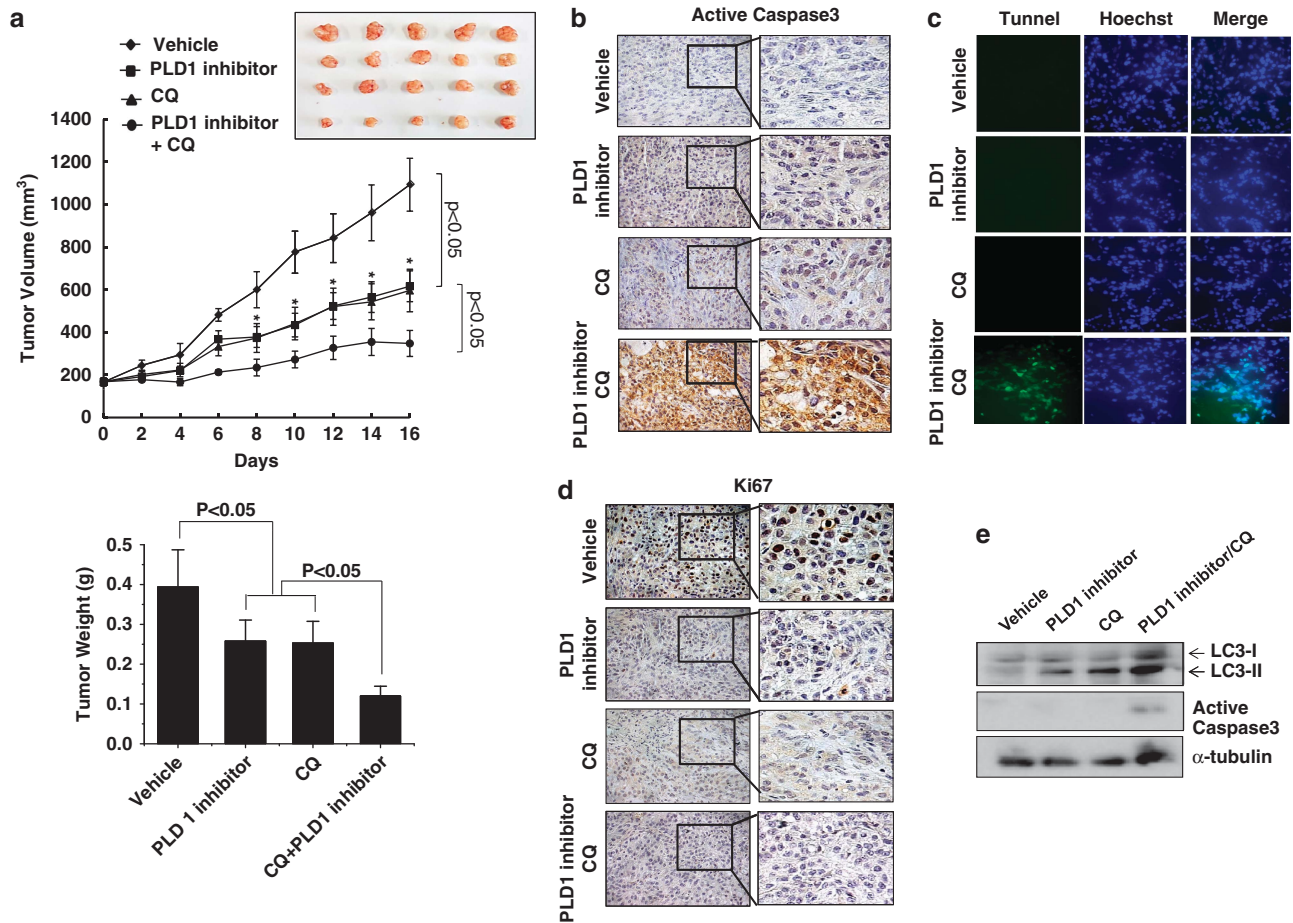
**Figure 8** PLD1 inhibitor synergizes with clinical inhibitor of autophagosome maturation to induce *in vivo* cancer regression and apoptosis. (**a**) Nude mice were injected subcutaneously with A549 cells ($5 \times 10^6$ cells). After 1 week, mice were subjected to intraperitoneal injection with PLD1 inhibitor (5 mg/kg) and/or CQ (10 mg/kg). The representative tumors from five mice are shown. The tumor volume of mice was measured with vernier calipers every two days (top). Representative tumors at the end of the experiment are shown. Tumor weight was also determined using an electronic scale (bottom). (**b–d**) Paraffin-embedded tumor sections were stained with antibody to active caspase, Ki67, and analyzed by TUNEL staining. (**e**) The lysates from tumor tissues were analyzed by immunoblot using the indicated antibody. Data are representative of three independent experiments

(Figure 8d). Similarly, combinational therapy led to greatly increased levels of LC3-II and active caspase-3 (Figure 8e). Considering the efficacy of combinational therapy using PLD1 inhibitor and CQ, small molecules targeting PLD1 may offer a translatable approach to cancer therapy in the future. Taken together, these findings demonstrate that PLD1 inhibitor synergizes with genetic inhibition of autophagy and clinical inhibitor of autophagosome maturation to induce apoptosis *in vivo*.

## Discussion

In the present study, we demonstrate PLD as a new player in the molecular machinery regulating autophagy. Modulation of autophagy may represent a new paradigm for cancer treatment that is relevant to both conventional cytotoxic drugs and targeted agents. The role of autophagy in cancer and treatment responsiveness is undoubtedly complicated. Although tumor cell susceptibility to autophagy may depend on tumor genotype and the therapeutic agents utilized, the available data are limited and it is not clear whether such a

strategy will be clinically beneficial.[36] The present study strongly suggests that PLD1 suppresses autophagy and that PLD1 inhibition augments the efficacy of anticancer regimens via facilitation of autophagic pathways. PLD2 also seems to have the same effect and thus it would appear that both PLDs are able to modulate autophagy. Overexpression of PLD has been reported to protect cancer cells from apoptosis,[37] and aberrant activation/expression of PLD has been widely implicated in a variety of cancers.[18,19]

PLD1 inhibition led to a great increase in the level of LC3-II protein in a variety of cells, and PA suppressed starvation-induced autophagy, suggesting that PLD activity has a negative role in autophagy. To assess whether LC3-II formation is altered by perturbation, one can assess its level in the presence of Baf A1, which inhibits LC3-II degradation by blocking autophagosome-lysosome fusion.[38] Therefore, differences in LC3-II levels in response to particular conditions in the presence of Baf A1 reflect changes in autophagosome synthesis. We demonstrated that PLD1 inhibition increased the on-rate of autophagy, at least *in vitro*. PLD1 knockdown-induced autophagy follows a canonical autophagic pathway

via *Atg1*(*Ulk1*), *Atg5* or *Atg7.* Given the critical role of mTOR signaling in regulation of autophagy, it is not be surprising to find that depletion and inhibition of PLD induces autophagy via suppression of mTOR. Expression of PLD1 abrogated the accumulation of GFP-LC3 dots observed in sphingosine kinase 1-overexpressing cells, which stimulate autophagy, whereas expression of catalytically inactive mutant of PLD1 did not inhibit autophagy induced by overexpression of sphingosine kinase 1.[39] On the contrary, the opposite effect of PLD1 on autophagy (i.e., positive regulation of autophagy through PLD1) has been reported.[40] A major difference between the findings of the study reported here and of that reported by Dall'Armi is the incubation time used when investigating autophagy in starved HeLa cells (6 *versus* 2 hs, respectively).[40] We observed that PLD1 suppressed autophagy flux both a shorter period (2 h) and long period (6 h, 12 h) of starvation. PLD1 activity was increased for 2 h of starvation and thereafter (6 h, 12 h) decreased. Thus, it seems that decreased activity of PLD1 for prolonged starvation promotes autophagy.

The proteolysis of long-lived proteins by macroautophagy is a standard, specific measure of autophagic degradation and represents an end-point assay for the pathway. We observed significant increase in the degradation of long-lived proteins in PLD1-depleted cells, indicating that knock-down of PLD1 stimulates the autophagic pathway.

Although activation of mTOR suppresses autophagy, PLD1 may function as both a positive and negative modulator of the autophagy pathway, depending on its subcellular localization, the cell state and the experimental conditions. p53 has also a dual role in autophagy regulation: p53 induces autophagy through mTOR inhibition[41] or transcriptional activation of the autophagy-inducing protein, DRAM,[42] in the context of DNA damage or p53 overexpression, whereas baseline or physiological levels of p53 can inhibit autophagy in other cellular contexts with enhanced mTOR activity by p53.[43] Thus, modulation of autophagy might be dependent on the cellular context. Such a dual role also has been described for Vps34, a lipid enzyme that is required for autophagy, but also stimulates mTOR.[44,45] Furthermore, it has been suggested that PLD1 has a novel role in transducing amino-acid signals to activate mTORC1 via the Vps34-phosphatidylinositol-3-phosphate-PLD1 pathway.[46] Thus, it is suggested that PLD1 might have a dual role on autophagy depending on cell contexts and its subcellular localization. Further studies will be required for understanding the mechanism for a dual role of PLD1 on autophagy.

The initiation step in the autophagy process is highly regulated, involving key signaling molecules that function as a macromolecular complex, the best characterized being the Beclin 1-Vps34, AMPK-ULK1 and ULK1-mTOR complexes.[38,47] Bcl2 is also involved in the inhibition of autophagy via binding to Beclin 1 and negatively regulating the autophagy-promoting Beclin 1/Vps34 complex.[14] Dissociation of Beclin 1 from Bcl-2, and thus activation of autophagy, in response to nutrient limitation depends on Bcl-2 phosphorylation by the starvation-activated JNK.[24] Our study suggests a model in which PLD1 inhibition promotes autophagy by releasing Beclin 1 from its association with Bc1-2 via phosphorylation of JNK to form a complex with

Vps34. PLD1 may be a critical regulator of autophagy by coordinating the major players of autophagy, the AMPK-mTOR-ULK1 and Vps34/Beclin 1 signaling pathways. Our results add to an increasingly complex homeostatic regulation in which mTOR and autophagy are interconnected.

Multiple studies have shown that genetic knockdown of Atgs or pharmacological inhibition of autophagy can effectively enhance tumor cell death induced by diverse anticancer drugs in preclinical models.[33] Although autophagy is a potential mechanism by which PLD1 inhibition restricts tumor growth, it may also provide temporary relief from the stress imposed by PLD1 inhibition. Rab9 GTPase, which regulates secretory and endocytic membrane traffic, is an essential protein for membrane expansion and fusion in alternative macroautophagy, but not in conventional macroautophagy.[48] Recently, it was suggested that macroautophagy can occur through at least two different pathways: an Atg5/Atg7-dependent pathway and an Atg5/Atg7-independent alternative non-canonical pathway.[48,49] Although lipidation of LC3 is accepted to be a good indicator of macroautophagy, it did not occur during the Atg5/Atg7-independent alternative macroautophagy. Unlike conventional macroautophagy, autophagosomes seemed to be generated in a Rab9-dependent manner by the fusion of the phagophore with vesicles derived from the trans-Golgi and late endosomes. Thus, macroautophagy is more complex than previously realized. Thus, it could be possible that PLD1 inhibition might sensitize death of Atg5/7-defective cells via Atg5/Atg7-independent pathways. We examined whether or not PLD1 inhibition induces Rab9-positive autophagic vacuolization by monitoring co-localization of RFP-Rab9 with Lamp-1, which is the late endosomal/lysosomal marker and not solely a marker of lysosomes. Interestingly, wild-type Rab9 but not dominant negative Rab9 (Rab9$^{S12N}$), colocalized with GFP-Lamp-1 under starvation condition (Supplementary Figure 12a), suggesting that PLD1 inhibition might induce Rab9-positive autophagic vacuolization. Next, we examined whether PLD1 regulates cell death via Rab9, independent of Atg5/7 pathway. Under starvation condition, Atg5$^{+/+}$ and Atg5$^{-/-}$ MEF were transfected with siRNA for Rab9, and then treated with PLD1 inhibitor. Knockdown of Rab9 showed much more resistance against PLD1 inhibitor-induced death of Atg5$^{-/-}$ MEF, compared with that of scrambled Rab9 (Supplementary Figures 12b and c), indicating that PLD1 inhibition can regulate cell death via Rab9-mediated pathway, which could be independent of autophagy. Although we do not provide any direct evidence for an alternative form of autophagy, it could be possible that alternative forms of autophagy do indeed have a role in the regulation of PLD1-mediated cell death. A direct evidence and more detailed picture of the pathophysiological relevance for alternative macroautophagy regulated by PLD should be investigated in the future study.

Lysosomotropic agents have shown anticancer activity either alone or in combination with other therapeutic agents.[32,35,50] PLD1 inhibition-induced autophagy can be exploited using lysosomotropic agents, such as the well-tolerated drug CQ, to promote cell death *in vitro* and tumor remission *in vivo*. The complex role of autophagy in tumorigenesis and treatment responsiveness makes it difficult to decipher how to universally modulate autophagy for

maximum therapeutic benefit, indicating that context- and cell type-specific approaches may be required. Thus, context-specific pharmacologic autophagy modulation holds great promise as a novel therapeutic approach, adding another weapon to the currently available armamentarium against cancer.

Indeed, our results suggest that blocking autophagy can be detrimental to cancer cell survival when autophagy is activated, providing a novel role for PLD in the molecular machinery regulating autophagy and rationale for a new therapeutic approach to enhance the anticancer efficacy of PLD inhibition.

## Materials and Methods

**Cell lines and materials.** HEK293, HeLa, A549, MCF10A, MDAMB231, DLD1, MEF, CHO and HN33 cells were cultured at 37 °C in DMEM (Invitrogen, Carlsbad, CA, USA) containing 10% fetal bovine serum and 1% antibiotic-antimycotic. ATG7-depleted MBA-MB231 stable cells were generated using shRNA for ATG7. Pld1 knockout mice were provided by Dr. G Paolo (Columbia University) and MEF were prepared. Tet-off Atg5 MEF were provided by Dr. N. Misushima (Tokyo Medical and Dental University), Atg5$^{+/+}$ andAtg5$^{-/-}$ RasV12/T-large antigen MEF were provided by Dr. G. Velasco (School of Biology, Complutense University), Atg7$^{+/+}$ and Atg7$^{-/-}$ MEF were provided by Dr. M. Komatsu (Tokyo Metropolitan Institute of Medical Science) and Ulk1$^{+/+}$ and Ulk1$^{-/-}$ MEF were provided by Dr. M. Kundu (St. Jude Children's Hospital). Cells were grown to 60% confluence for transient transfection using Lipofectamine Plus (Invitrogen) according to the manufacturer's instructions. PLD1 inhibitor (VU0155069) was purchased from Cayman Chemical (AnnArbor, MI, USA). CQ and bafilomycin1 (Baf A1) were obtained from Sigma (Beverly, MA, USA). The siRNAs of corresponding to human PLD1 sequences (nucleotides 1571–1591, 5′-AAGGUGGGACGACAAUGAGCA-3′).

**PLD activity assay.** For measurement of PLD activity, cells were labeled with [$^3$H]myristic acid, and PLD activity was assessed by measurement of the formation of [$^3$H]phosphatidylbutanol, the product of PLD-mediated transphosphatidylation, in the presence of 1-butanol, as previously described.[51]

**Western blotting and immunoprecipitation.** Cell lysates were analyzed by immunoblot and/or immunoprecipitation as previously described.[52] Enhanced chemiluminescence was used for signal detection. The following antibodies were used: anti-tubulin (Sigma), anti-GFP (Santa Cruz Biotechnology, Santa Cruz, CA, USA), anti-active caspase3 (Cell Signaling, Danvers, MA, USA), Ki67 (Cell Signaling), phospho-mTOR (Ser2448, Cell Signaling), phospho-S6K1 (Thr389, Cell Signaling), phospho-AMPK (Thr172, Cell Signaling), AMPK (Cell Signaling), LC3B (Cell Signaling), p62 (Cell Signaling), phospho-ULK1 (Ser555/Ser757, Cell Signaling), ULK1 (Cell Signaling), ATG5 (Santa Cruz Biotechnology) and ATG7 (Abcam, Cambridge, MA, USA). Rabbit polyclonal anti-PLD antibody that recognizes both PLD1 and PLD2 were generated as previously described.[37]

**Fluorescence microscopy.** Cells were transfected with various PLD1 constructs and incubated with media containing 1 mg/ml Hoechst (Invitrogen) for 20 min. Cells were visualized and the images were collected using a fluorescence microscope (Axiovert200 M, Zeiss, Wetzlar, Germany) and a confocal fluorescence microscope (LXM510, Zeiss).

**Autophagy analysis by LC3 monitoring.** To monitor the formation of GFP-LC3 puncta, cells were transiently transfected with GFP-LC3 and then cultured under nutrient starvation conditions such as on HBSS (Hank's Buffered Salt Solution; amino acid-free medium).The cells were then fixed with 4% paraformaldehyde for fluorescence microscopy. Quantification of autophagic vacuoles was analyzed by calculating the numbers of LC3 puncta (endogenous LC3, RFP-LC3, RFP + /GFP + LC3 or RFP + /GFP − LC3 from some fields containing more than 3–5 randomly selected cells in the microscopy-captured images). RFP-LC3 was provided by Dr. Colombo (Universidad Nacional de Cuyo, Mendoza, Argentina) and mRFP-GFP-LC3 was provided by Dr. T. Yoshimori (Research Institute for Microbial Diseases, Osaka University). LC3$^{WT}$ and LC3$^{G120A}$ were kindly provided by Dr. Marja Jäättelä (Apoptosis Department and Centre for Genotoxic Stress Research, Denmark).

**Cell death analysis.** Cell death was measured by staining with PI (1 $\mu$g/ml, Invitrogen) that was added directly to the culture medium. Cells were photographed under both phase contrast and fluorescent conditions. The PI-positive cells were expressed as a percentage of the total number of cells (200 counted under phase contrast).

**Electron microscopy.** The material was pre-fixed with 2.5% glutaraldehyde (4 °C, phosphate buffer, pH 7.2) and post-fixed with 1% osmuim tetroxide in the same buffer. The material was then dehydrated with a series of the graded ethyl alcohol and embedded in epoxy resin (Epon 812 mixture). Thick sections (1 $\mu$m) were subsequently stained with 1% toluidine blue for light microscopy. In addition, thin sections (50–60 nm) were prepared using an ultramicrotome (Leica, Reichert SuperNova, Heidelberg, Germany), double stained with uranyl acetate and lead citrate and then examined using a transmission electron microscope (JEM1200EX-II, JEOL, Tokyo, Japan).

**Xenograft study.** A mouse xenograft model was established using 6-week old BALB/c nude mice (Central Lab Animal Inc., Seoul, Korea). Tumor cells (5 × 10$^6$ Ras/T-antigen-MEF transformed or A549 cells) were suspended in 0.1 ml of serum-free medium and then injected subcutaneously into the upper flank of each nude mouse. Two weeks after inoculation, CQ (10 mg/kg) and/or PLD1 inhibitor (5 mg/kg) were subjected to intraperitoneal injection three times a week. After xenografts started growing, the volume and weight of the tumors were measured. The animal protocol used in this study was reviewed by the Pusan National University–Institutional Animal Care and Use Committee for ethical procedures and scientific care and approved (approval number PNU-2009- 0024).

**Immunohistochemistry.** The paraffin-embedded sections were cleared and each section was deparaffinized by three changes of xylene for 5 min each, rehydrated in a graded series of ethanol (100–70%) and then washed with tap water. After hydration in PBS, endogenous peroxidase was depleted with 0.3% H$_2$O$_2$ for 10 min at room temperature. The samples were then blocked with 3% H$_2$O$_2$ for 10 min and washed with PBS several times. After washing, the samples were further blocked with normal horse serum for 10 min at room temperature and then incubated first with specific antibody, then with secondary antibodies. Next, the samples were biotinylated and visualized by the avidin-biotinylated enzyme complex (ABC) technique using the Vectastain ABC kit (Vector Laboratories, Burlingame, CA, USA) and subsequent 3,3-diaminobenzidine (DAB) staining (DAB substrate kit, Vector Laboratories), followed by counterstaining of the nuclei with hematoxylin. The primary antibodies were performed using LC3B (Cell signaling), active caspase3 (Santa Cruz Biotechnology, CA, USA) and Ki67 (Abcam). Tissue TUNEL assays were performed using an ApopTag Peroxidase In Situ Apoptosis Detection Kit (Millipore, Billerica, MA, USA).

**Statistical analysis.** Results are expressed as the mean ± S.D. of the number of determinations indicated. Statistical significance of differences was determined by analysis of variance. A $P$ <0.01 was considered to indicate significance.

## Conflict of Interest
The authors declare no conflict of interest.

1. Mathew R, Karantza-Wadsworth V, White E. Role of autophagy in cancer. *Nat Rev Cancer* 2007; **7**: 961–967.
2. Tanida I, Ueno T, Kominami E. LC3 conjugation system in mammalian autophagy. *Int J Biochem Cell Biol* 2004; **36**: 2503–2518.

3. Mizushima N, Yoshimori T, Levine B. Methods in mammalian autophagy research. *Cell* 2010; **140**: 313–326.
4. Kuma A, Hatano M, Matsui M, Yamamoto A, Nakaya H, Yoshimori T *et al.* The role of autophagy during the early neonatal starvation period. *Nature* 2004; **432**: 1032–1036.
5. Levine B, Kroemer G. Autophagy in the pathogenesis of disease. *Cell* 2008; **132**: 27–42.
6. Chen N, Debnath J. Autophagy and tumorigenesis. *FEBS Lett* 2010; **584**: 1427–1435.
7. Degenhardt K, Mathew R, Beaudoin B, Bray K, Anderson D, Chen G *et al.* Autophagy promotes tumor cell survival and restricts necrosis, inflammation, and tumorigenesis. *Cancer Cell* 2006; **10**: 51–64.
8. Chen N, Karantza V. Autophagy as a therapeutic target in cancer. *Cancer Biol Ther* 2011; **11**: 157–168.
9. Kuma A, Mizushima N. Physiological role of autophagy as an intracellular recycling system: with an emphasis on nutrient metabolism. *Semin Cell Dev Biol* 2010; **21**: 683–690.
10. Efeyan A, Sabatini DM. mTOR and cancer: many loops in one pathway. *Curr Opin Cell Biol* 2010; **22**: 169–176.
11. Kim J, Kundu M, Viollet B, Guan KL. AMPK and mTOR regulate autophagy through direct phosphorylation of Ulk1. *Nat Cell Biol* 2011; **13**: 132–141.
12. Egan DF, Shackelford DB, Mihaylova MM, Gelino S, Kohnz RA, Mair W *et al.* Phosphorylation of ULK1 (hATG1) by AMP-activated protein kinase connects energy sensing to mitophagy. *Science* 2011; **331**: 456–461.
13. Funderburk SF, Wang QJ, Yue Z. The Beclin 1-VPS34 complex–at the crossroads of autophagy and beyond. *Trends Cell Biol* 2010; **20**: 355–362.
14. Pattingre S, Tassa A, Qu X, Garuti R, Liang XH, Mizushima N *et al.* Bcl-2 antiapoptotic proteins inhibit Beclin 1-dependent autophagy. *Cell* 2005; **122**: 927–939.
15. Wei Y, Pattingre S, Sinha S, Bassik M, Levine B. JNK1-mediated phosphorylation of Bcl-2 regulates starvation-induced autophagy. *Mol Cell* 2008; **30**: 678–688.
16. Foster DA. Regulation of mTOR by phosphatidic acid? *Cancer Res* 2007; **67**: 1–4.
17. Sun Y, Chen J. mTOR signaling: PLD takes center stage. *Cell Cycle* 2008; **7**: 3118–3123.
18. Kang DW, Choi KY, Min do S. Phospholipase D meets Wnt signaling: a new target for cancer therapy. *Cancer Res* 2011; **71**: 293–297.
19. Huang P, Frohman MA. The potential for phospholipase D as a new therapeutic target. *Expert Opin Ther Targets* 2007; **11**: 707–716.
20. Mathew R, Karp CM, Beaudoin B, Vuong N, Chen G, Chen HY *et al.* Autophagy suppresses tumorigenesis through elimination of p62. *Cell* 2009; **137**: 1062–1075.
21. Kimura S, Noda T, Yoshimori T. Dissection of the autophagosome maturation process by a novel reporter protein, tandem fluorescent-tagged LC3. *Autophagy* 2007; **3**: 452–460.
22. Farkas T, Hoyer-Hansen M, Jaattela M. Identification of novel autophagy regulators by a luciferase-based assay for the kinetics of autophagic flux. *Autophagy* 2009; **5**: 1018–1025.
23. Frankel LB, Wen J, Lees M, Hoyer-Hansen M, Farkas T, Krogh A *et al.* microRNA-101 is a potent inhibitor of autophagy. *EMBO J* 2011; **30**: 4628–4641.
24. Hosokawa N, Hara Y, Mizushima N. Generation of cell lines with tetracycline-regulated autophagy and a role for autophagy in controlling cell size. *FEBS Lett* 2007; **581**: 2623–2629.
25. Komatsu M, Waguri S, Ueno T, Iwata J, Murata S, Tanida I *et al.* Impairment of starvation-induced and constitutive autophagy in Atg7-deficient mice. *J Cell Biol* 2005; **169**: 425–434.
26. Faivre S, Kroemer G, Raymond E. Current development of mTOR inhibitors as anticancer agents. *Nat Rev Drug Discov* 2006; **5**: 671–688.
27. Meley D, Bauvy C, Houben-Weerts JH, Dubbelhuis PF, Helmond MT, Codogno P *et al.* AMP-activated protein kinase and the regulation of autophagic proteolysis. *J Biol Chem* 2006; **281**: 34870–34879.
28. Kang R, Zeh HJ, Lotze MT, Tang D. The Beclin 1 network regulates autophagy and apoptosis. *Cell Death Differ* 2011; **18**: 571–580.
29. Zeng X, Overmeyer JH, Maltese WA. Functional specificity of the mammalian Beclin-Vps34 PI 3-kinase complex in macroautophagy *versus* endocytosis and lysosomal enzyme trafficking. *J Cell Sci* 2006; **119**: 259–270.

30. Furuya N, Yu J, Byfield M, Pattingre S, Levine B. The evolutionarily conserved domain of Beclin 1 is required for Vps34 binding, autophagy and tumor suppressor function. *Autophagy* 2005; **1**: 46–52.
31. White E, DiPaola RS. The double-edged sword of autophagy modulation in cancer. *Clin Cancer Res* 2009; **15**: 5308–5316.
32. Carew JS, Nawrocki ST, Kahue CN, Zhang H, Yang C, Chung L *et al.* Targeting autophagy augments the anticancer activity of the histone deacetylase inhibitor SAHA to overcome Bcr-Abl-mediated drug resistance. *Blood* 2007; **110**: 313–322.
33. Yang ZJ, Chee CE, Huang S, Sinicrope FA. The role of autophagy in cancer: therapeutic implications. *Mol Cancer Ther* 2011; **10**: 1533–1541.
34. Salazar M, Carracedo A, Salanueva IJ, Hernandez-Tiedra S, Lorente M, Egia A *et al.* Cannabinoid action induces autophagy-mediated cell death through stimulation of ER stress in human glioma cells. *J Clin Invest* 2009; **119**: 1359–1372.
35. Amaravadi RK, Yu D, Lum JJ, Bui T, Christophorou MA, Evan GI *et al.* Autophagy inhibition enhances therapy-induced apoptosis in a Myc-induced model of lymphoma. *J Clin Invest* 2007; **117**: 326–336.
36. Yang ZJ, Chee CE, Huang S, Sinicrope F. Autophagy modulation for cancer therapy. *Cancer Biol Ther* 2011; **11**: 169–176.
37. Kim J, Lee YH, Kwon TK, Chang JS, Chung KC, Min DS. Phospholipase D prevents etoposide-induced apoptosis by inhibiting the expression of early growth response-1 and phosphatase and tensin homologue deleted on chromosome 10. *Cancer Res* 2006; **66**: 784–793.
38. Rubinsztein DC, Cuervo AM, Ravikumar B, Sarkar S, Korolchuk V, Kaushik S *et al.* In search of an 'autophagomometer'. *Autophagy* 2009; **5**: 585–589.
39. Lavieu G, Scarlatti F, Sala G, Carpentier S, Levade T, Ghidoni R *et al.* Regulation of autophagy by sphingosine kinase 1 and its role in cell survival during nutrient starvation. *J Biol Chem* 2006; **281**: 8518–8527.
40. Dall'Armi C, Hurtado-Lorenzo A, Tian H, Morel E, Nezu A, Chan R *et al.* The phospholipase D1 pathway modulates macroautophagy. *Nat Commun* 2010; **1**: 142.
41. Feng Z, Zhang H, Levine AJ, Jin S. The coordinate regulation of the p53 and mTOR pathways in cells. *Proc Natl Acad Sci USA* 2005; **102**: 8204–8209.
42. Crighton D, Wilkinson S, O'Prey J, Syed N, Smith P, Harrison PR *et al.* DRAM, a p53-induced modulator of autophagy, is critical for apoptosis. *Cell* 2006; **126**: 121–134.
43. Tasdemir E, Maiuri MC, Galluzzi L, Vitale I, Djavaheri-Mergny M, D'Amelio M *et al.* Regulation of autophagy by cytoplasmic p53. *Nat Cell Biol* 2008; **10**: 676–687.
44. Backer JM. The regulation and function of class III PI3Ks: novel roles for Vps34. *Biochem J* 2008; **410**: 1–17.
45. Pattingre S, Espert L, Biard-Piechaczyk M, Codogno P. Regulation of macroautophagy by mTOR and Beclin 1 complexes. *Biochimie* 2008; **90**: 313–323.
46. Yoon MS, Du G, Backer JM, Frohman MA, Chen J. Class III PI-3-kinase activates phospholipase D in an amino acid-sensing mTORC1 pathway. *J Cell Biol* 2011; **195**: 435–447.
47. Xie Z, Klionsky DJ. Autophagosome formation: core machinery and adaptations. *Nat Cell Biol* 2007; **9**: 1102–1109.
48. Nishida Y, Arakawa S, Fujitani K, Yamaguchi H, Mizuta T, Kanaseki T *et al.* Discovery of Atg5/Atg7-independent alternative macroautophagy. *Nature* 2009; **461**: 654–658.
49. Shimizu S, Arakawa S, Nishida Y. Autophagy takes an alternative pathway. *Autophagy* 2010; **6**: 290–291.
50. Degtyarev M, De Maziere A, Orr C, Lin J, Lee BB, Tien JY *et al.* Akt inhibition promotes autophagy and sensitizes PTEN-null tumors to lysosomotropic agents. *J Cell Biol* 2008; **183**: 101–116.
51. Jang YH, Ahn BH, Namkoong S, Kim YM, Jin JK, Kim YS *et al.* Differential regulation of apoptosis by caspase-mediated cleavage of phospholipase D isozymes. *Cell Signal* 2008; **20**: 2190–2207.
52. Jang YH, Min do S. Nuclear localization of phospholipase D1 mediates the activation of nuclear protein kinase C(alpha) and extracellular signal-regulated kinase signaling pathways. *J Biol Chem* 2011; **286**: 4680–4689.